Article

Polyplexes from Poly(aspartamide) Bearing 1,2-Diaminoethane Side Chains Induce pH-Selective, Endosomal Membrane Destabilization with Amplified Transfection and Negligible Cytotoxicity

Kanjiro Miyata, Makoto Oba, Masataka Nakanishi, Shigeto Fukushima, Yuichi Yamasaki, Hiroyuki Koyama, Nobuhiro Nishiyama, and Kazunori Kataoka

J. Am. Chem. Soc., **2008**, 130 (48), 16287-16294 • DOI: 10.1021/ja804561g • Publication Date (Web): 12 November 2008

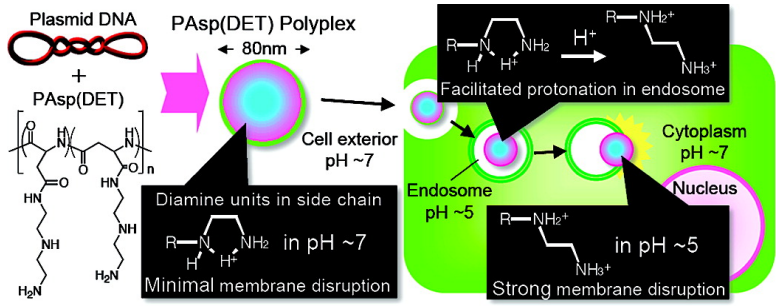

More About This Article

Additional resources and features associated with this article are available within the HTML version:

- Supporting Information
- Access to high resolution figures
- Links to articles and content related to this article
- Copyright permission to reproduce figures and/or text from this article

View the Full Text HTML

J|A|C|S
ARTICLES

Published on Web 11/12/2008

Polyplexes from Poly(aspartamide) Bearing 1,2-Diaminoethane Side Chains Induce pH-Selective, Endosomal Membrane Destabilization with Amplified Transfection and Negligible Cytotoxicity

Kanjiro Miyata,[†,‡] Makoto Oba,[§] Masataka Nakanishi,[||] Shigeto Fukushima,[⊥] Yuichi Yamasaki,[||,‡] Hiroyuki Koyama,[§] Nobuhiro Nishiyama,[⊥,‡] and Kazunori Kataoka*[,†,||,⊥,‡]

Department of Bioengineering and Department of Materials Engineering, Graduate School of Engineering, and Center for NanoBio Integration, The University of Tokyo, 7-3-1 Hongo, Bunkyo-ku, Tokyo 113-8656, Japan, Department of Clinical Vascular Regeneration, Graduate School of Medicine, The University of Tokyo, 7-3-1 Hongo, Bunkyo-ku, Tokyo 113-8655, Japan, and Center for Disease Biology and Integrative Medicine, Graduate School of Medicine, The University of Tokyo, 7-3-1 Hongo, Bunkyo-ku, Tokyo 113-0033, Japan

Received June 23, 2008; E-mail: kataoka@bmw.t.u-tokyo.ac.jp

Abstract: Polyplexes assembled from poly(aspartamide) derivatives bearing 1,2-diaminoethane side chains, [PAsp(DET)] display amplified in vitro and in vivo transfection activity with minimal cytotoxicity. To elucidate the molecular mechanisms involved in this unique function of PAsp(DET) polyplexes, the physicochemical and biological properties of PAsp(DET) were thoroughly evaluated with a control bearing 1,3-diaminopropane side chains, PAsp(DPT). Between PAsp(DET) and PAsp(DPT) polyplexes, we observed negligible physicochemical differences in particle size and ζ-potential. However, the one methylene variation between 1,2-diaminoethane and 1,3-diaminopropane drastically altered the transfection profiles. In sharp contrast to the constantly high transfection efficacy of PAsp(DET) polyplexes, even in regions of excess polycation to plasmid DNA (pDNA) (high N/P ratio), PAsp(DPT) polyplexes showed a significant drop in the transfection efficacy at high N/P ratios due to the progressively increased cytotoxicity with N/P ratio. The high cytotoxicity of PAsp(DPT) was closely correlated to its strong destabilization effect on cellular membrane estimated by hemolysis, leakage assay of cytoplasmic enzyme (LDH assay), and confocal laser scanning microscopic observation. Interestingly, PAsp(DET) revealed minimal membrane destabilization at physiological pH, yet there was significant enhancement in the membrane destabilization at the acidic pH mimicking the late endosomal compartment (pH $\sim$5). Apparently, the pH-selective membrane destabilization profile of PAsp(DET) corresponded to a protonation change in the flanking diamine unit, i.e., the monoprotonated gauche form at physiological pH and diprotonated anti form at acidic pH. These significant results suggest that the protonated charge state of 1,2-diaminoethane may play a substantial role in the endosomal disruption. Moreover, this novel approach for endosomal disruption neither perturbs the membranes of cytoplasmic vesicles nor organelles at physiological pH. Thus, PAsp(DET) polyplexes, residing in late endosomal or lysosomal states, smoothly exit into the cytoplasm for successful transfection without compromising cell viability.

Introduction

Successful transfection with polycation-based gene vectors (polyplexes) significantly depends on the chemical structure of the incorporated polycations.[1,2] Polyethylenimine (PEI) and its derivatives display protonation of amino groups over a wide pH range. Following polyplex formation, these well-known polycations exert a high transfection efficacy through endosomal escape supported by the proton sponge hypothesis.[3,4] However, there remains a great concern for the availability of PEI-based polyplexes in translational research, mainly due to their problematic toxicity.[5,6] Thus, the rational design of a polyplex system exhibiting clinically relevant gene expression with minimal toxicity remains an urgent complication for clinical

[†] Department of Bioengineering.
[‡] Center for NanoBio Integration.
[§] Department of Clinical Vascular Regeneration.
[||] Department of Materials Engineering.
[⊥] Center for Disease Biology and Integrative Medicine.

(1) Pack, D. W.; Hoffman, A. S.; Pun, S.; Stayton, P. S. *Nature Rev. Drug Discovery* **2005**, *4*, 581–593.
(2) Mastrobattista, E.; van der Aa, M. A. E. M.; Hennink, W. E.; Crommelin, D. J. A. *Nature Rev. Drug Discovery* **2006**, *5*, 115–121.
(3) Boussif, O.; Lezoualc'h, F.; Zanta, M. A.; Mergny, M. D.; Scherman, D.; Demeneix, B.; Behr, J. *Proc. Natl. Acad. Sci. U.S.A.* **1995**, *92*, 7297–7301.
(4) Neu, M.; Fischer, D.; Kissel, T. *J. Gene Med.* **2005**, *7*, 992–1009.
(5) Fischer, D.; Li, Y.; Ahlemeyer, B.; Krieglstein, J.; Kissel, T. *Biomaterials* **2003**, *24*, 1121–1131.
(6) Moghimi, S. M.; Symonds, P.; Murray, J. C.; Hunter, A. C.; Debska, G.; Szewczyk, A. *Mol. Ther.* **2005**, *11*, 990–995.

extension of nonviral gene vectors. To overcome polycationic toxicity, a promising strategy is the incorporation of hydrophilic and nonionic poly(ethylene glycol) (PEG) to shield the deleterious, excess cationic charge associated with these carriers. Indeed, PEGylated polyplexes (polyplex micelles) formed through the association of PEG−polycation copolymers with DNA[7−12] were biocompatible under in vivo conditions, leading to appreciable in vivo gene expression with lower toxic effects.[13−16]

Nevertheless, further improvements in polyplex micelle systems are needed to show higher transfection efficacy and lower cytotoxicity for clinical translation. This recurring and pervasive problem endures, thereby motivating studies devoted to modulate the micellar, polycationic structure for effective clinical application in human gene therapy. Recently, we found that a flanking benzyl ester group of PEG-*b*-poly(*β*-benzyl L-aspartate) (PBLA) underwent a quantitative aminolysis reaction with a variety of amine compounds under a very mild condition,[17] allowing us to prepare an N-substituted poly(aspartamide) (PAsp) derivative library possessing a variety of cationic side chains from a single platformed PBLA.[18−25] A series of transfection and cytotoxicity assays of polyplexes prepared from the N-substituted PAsp derivative library revealed a highly promising candidate, PEG-*b*-poly{*N*-[*N*-(2-aminoethyl)-2-aminoethyl]aspartamide} (PEG−PAsp(DET)). A 1,2-diaminoethane unit was introduced as a side chain into PEG-*b*-PAsp, forming PEG-*b*-PAsp(DET); a series of primary cells and cultured cell lines were transfected, and significant gene expression with limited cytotoxicity was obtained. PEG−*b*-PAsp(DET) displayed high transfection efficacy comparable to commercially available linear PEI (ExGen 500) and the lipid-based system (Lipofectamine 2000); moreover, cytotoxicity levels were substantially lower compared to the controls.[15,16,19,21−25] Furthermore, PEG−PAsp(DET) polyplex micelles were successfully transfected in two animal models: (i) a rabbit's clamped carotid artery with neointima via intra-arterial injection[15] and (ii) a mouse skull by regulated release from a calcium phosphate cement scaffold to induce bone regeneration through the differentiation factor transduction.[16] The success of PEG−PAsp (DET) gene delivery in vivo has been attributed to the unique 1,2-diaminoethane structure in the side chain, where the *N*-(2-aminoethyl)-2-aminoethyl group exhibits a distinctive two-step protonation behavior. This dual protonation state suggests a strong pH-buffering capacity of Asp(DET) units for efficient endosomal escape.[19,21] Nevertheless, it still remains unknown whether the protonation behavior provides the crucial factor for excellent transfection when incorporated with PEG−PAsp. In parallel, it is unclear whether the low cytotoxicity of PEG−PAsp (DET) polyplex micelles is related to the particular cationic structure of Asp(DET) or simply due to the biocompatible PEG outer layer of the polyplex micelles.

These issues motivated us to clarify the structural factor of PAsp(DET) on transfection efficacy as well as cytocompatibility for additional polycationic structures successful for human gene therapy. To properly address the many architectural and chemical contributions of PEG−PAsp(DET), the following poly(aspartamides) were employed: (i) PAsp(DET) homopolymers to elucidate the effect of Asp(DET) units without PEGylation and (ii) a poly(aspartamide) bearing 1,3-diaminopropane units in the side chain as a control for 1,2-diaminoethane units, poly{*N*-[*N*-(3-aminopropyl)-3-aminopropyl]aspartamide} [PAsp(DPT)]. PAsp(DPT) exhibited a protonation degree over 88% at physiological pH and was considered to have a weak proton sponge effect. The high protonated state of Asp(DPT) at physiological pH is explained by the lowered electrostatic repulsion between the protonated diamine side chain units by the additional methylene group compared to Asp(DET). Detailed analysis of cellular membrane destabilization by PAsp(DET) and PAsp(DPT) revealed the distinct behavior of PAsp(DET) to facilitate membrane destabilization at the acidic pH of late endosomal or lysosomal states. This pH-selective membrane destabilization allows endosomal escape of PAsp(DET) polyplexes into the cytoplasm with limited toxicity to the other cytoplasmic membranes lying at neutral pH.

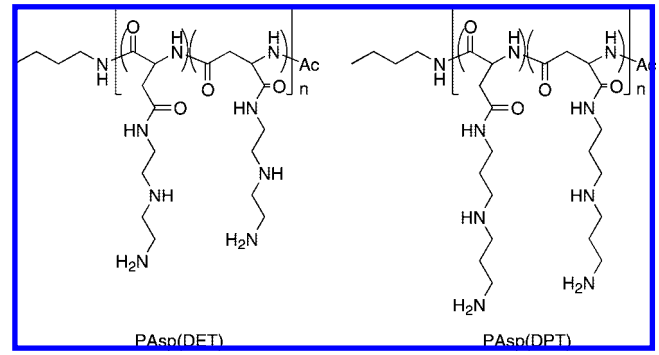

Results and Discussion

Protonation Degree (α) and Apparent pK_a of PAsp(DET) and PAsp(DPT). Previous studies revealed that a high transfection efficacy of PEI-based polyplexes was ascribed to their efficient endosomal escape, possibly due to the increased

(7) Kakizawa, Y.; Kataoka, K. *Adv. Drug Delivery Rev.* **2002**, *54*, 203–222.
(8) Katayose, S.; Kataoka, K. *Bioconjugate Chem.* **1997**, *8*, 702–707.
(9) Wolfert, M. A.; Schacht, E. H.; Toncheva, V.; Ulbrich, K.; Nazarova, O.; Seymour, L. W. *Human Gene Ther.* **1996**, *10*, 2123–2133.
(10) Choi, Y. H.; Liu, F.; Kim, J.; Choi, Y. K.; Park, J. S.; Kim, S. W. *J. Controlled Release* **1998**, *54*, 39–48.
(11) Vinogradov, S. V.; Bronich, T. K.; Kabanov, A. V. *Bioconjugate Chem.* **1998**, *9*, 805–812.
(12) Blessing, T.; Kursa, M.; Holzhauser, R.; Kircheis, R.; Wagner, E. *Bioconjugate Chem.* **2001**, *12*, 529–537.
(13) Harada-Shiba, M.; Yamauchi, K.; Harada, A.; Takamisawa, I.; Shimokado, K.; Kataoka, K. *Gene Ther.* **2002**, *9*, 407–414.
(14) Miyata, K.; Kakizawa, Y.; Nishiyama, N.; Yamasaki, Y.; Watanabe, T.; Kohara, M.; Kataoka, K. *J. Controlled Release* **2005**, *109*, 15–23.
(15) Akagi, D.; Oba, M.; Koyama, H.; Nishiyama, N.; Fukushima, S.; Miyata, T.; Nagawa, H.; Kataoka, K. *Gene Ther.* **2007**, *14*, 1029–1038.
(16) Itaka, K.; Ohba, S.; Miyata, K.; Kawaguchi, H.; Nakamura, K.; Takato, T.; Chung, U.; Kataoka, K. *Mol. Ther.* **2007**, *15*, 1655–1662.
(17) Nakanishi, M.; Park, J.-S.; Jang, W.-D.; Oba, M.; Kataoka, K. *React. Funct. Polym.* **2007**, *67*, 1361–1372.
(18) Fukushima, S.; Miyata, K.; Nishiyama, N.; Kanayama, N.; Yamasaki, Y.; Kataoka, K. *J. Am. Chem. Soc.* **2005**, *127*, 2810–2811.
(19) Kanayama, N.; Fukushima, S.; Nishiyama, N.; Itaka, K.; Jang, W.-D.; Miyata, K.; Yamasaki, Y.; Chung, U.; Kataoka, K. *ChemMedChem.* **2006**, *1*, 439–444.
(20) Arnida,; Nishiyama, N.; Kanayama, N.; Jang, W.-D.; Yamasaki, Y.; Kataoka, K. *J. Controlled Release* **2006**, *115*, 208–215.
(21) Han, M.; Bae, Y.; Nishiyama, N.; Miyata, K.; Oba, M.; Kataoka, K. *J. Controlled Release* **2007**, *121*, 38–48.
(22) Miyata, K.; Fukushima, S.; Nishiyama, N.; Yamasaki, Y.; Kataoka, K. *J. Controlled Release* **2007**, *122*, 252–260.
(23) Masago, K.; Itaka, K.; Nishiyama, N.; Chung, U.; Kataoka, K. *Biomaterials* **2008**, *28*, 5169–5175.
(24) Takae, S.; Miyata, K.; Oba, M.; Ishii, T.; Nishiyama, N.; Itaka, K.; Yamasaki, Y.; Koyama, H.; Kataoka, K. *J. Am. Chem. Soc.* **2008**, *130*, 6001–6009.
(25) Lee, Y.; Miyata, K.; Oba, M.; Ishii, T.; Fukushima, S.; Han, M.; Koyama, H.; Nishiyama, N.; Kataoka, K. *Angew. Chem., Int. Ed.* **2008**, *47*, 5163–5166.

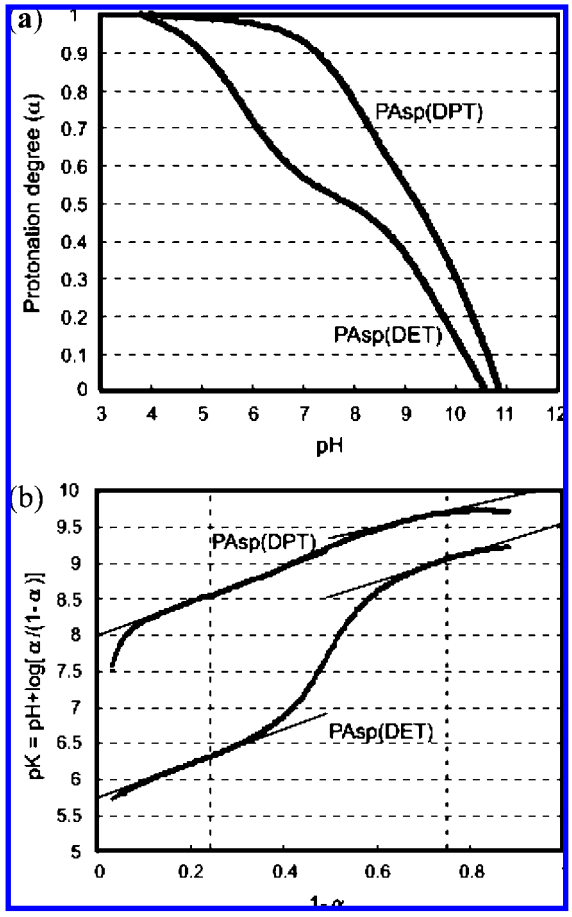

Figure 1. Protonation behavior of PAsp(DET) and PAsp(DPT). (a) Change in protonation degree (α) with pH (α/pH curve) (150 mM NaCl, 37 °C). (b) Change in apparent pK with $1 - \alpha$ [pK/$(1 - \alpha)$ curve].

osmotic pressure caused by facilitated protonation of polycations in endosomal acidic compartments (the proton sponge effect).[3,4] Hence, the difference in the protonation degree between neutral pH and endosomal acidic pH (from 7.4 to 5.0) has been considered to be a crucial factor for successful transfection with polycation-based systems. In this regard, the α of PAsp(DET) and PAsp(DPT) was estimated from the potentiometric titration, which was monitored over the range of pH 2.3−12 in the 150 mM NaCl solution at 37 °C, mimicking the physiological condition. As shown in Figure 1a, the α/pH curves calculated from the obtained titration curves (data not shown) revealed that the protonation behavior of the cationic poly(aspartamides) fairly depended on the number of methylene groups between the primary and secondary amino groups in the side chain. PAsp(DET) exhibited a substantial change in the α from neutral pH 7.4 to acidic pH 5.0 due to a distinctive two-step protonation behavior; i.e., 37% increase in the α through the pH drop from 7.4 to 5.0. In contrast, PAsp(DPT) showed facilitated protonation typically at physiological pH, and consequently, the increase in the α by changing pH from 7.4 to 5.0 was only 10%, an approximately 4 times smaller value than that expected for PAsp(DET). These results indicate that PAsp(DET) has potentially higher buffering capacity in endosomal acidic compartments than PAsp(DPT).

From the distinctive two-step protonation behavior of PAsp(DET), it is reasonably concluded that the first and the second protonation in the side chain proceeds separately. The remarkable difference in the protonation behavior between PAsp(DET) and PAsp(DPT) in the region of $0.5 < \alpha < 1$ indicates that the 1,2-diaminoethane unit in PAsp(DET) has restricted second protonation compared to the 1,3-diaminopropane unit in PAsp(DPT). The pK (=pH + log[α/(1 − α)]) values of PAsp(DET) and PAsp(DPT) were then calculated and plotted against $1 - \alpha$. Figure 1b clearly displays that PAsp(DET) has a substantially lower pK value in the range of $0 < 1 - \alpha < 0.5$, corresponding to the second protonation, than PAsp(DPT). Herein, apparent pK_a values in the first and the second protonations were defined as pK_{a1} (α = 0.25) and pK_{a2} (α = 0.75), respectively, and eventually were determined as follows: p$K_{a1,DET}$ = 9.1 and p$K_{a2,DET}$ = 6.3 for PAsp(DET), and p$K_{a1,DPT}$ = 9.7 and p$K_{a2,DPT}$ = 8.6 for PAsp(DPT). Although a large difference was not observed for K_{a1}, 2 orders of magnitude difference was observed for K_{a2}. It is worth noting that p$K_{a2,DET}$ was much lower than p$K_{a1,DET}$, indicating that the diprotonated form of the PAsp(DET) side chain suffers a thermodynamic penalty, presumably due to the electrostatic repulsion between two charged amino groups in the 1,2-diaminoethane moiety. The available conformation may be limited to an anti form according to three-bond interaction, i.e., butane effect, as shown in Scheme 1 to minimize the steric as well as electrostatic repulsion. As a result, the 1,2-diaminoethane side chain in PAsp(DET) takes a monoprotonated form at physiological pH (α = 0.53 at pH 7.4) as calculated from Figure 1a. Alternatively, addition of a single, hydrophobic methylene group in 1,3-diaminopropane units reduces the repulsion between the charged amino groups to increase the conformational freedom, leading to the smooth second protonation in PAsp(DPT) (α = 0.88 at pH 7.4). Note that both the 1,2-diaminoethane and 1,3-diaminopropnae, in PAsp(DET) and PAsp(DPT), respectively, may prefer to take the gauche conformation at the monoprotonated state, which is supported from the molecular orbital calculation.[26,27]

Scheme 1. Two-Step Protonation of the 1,2-Diaminoethane Moiety in the Side Chain of PAsp(DET)

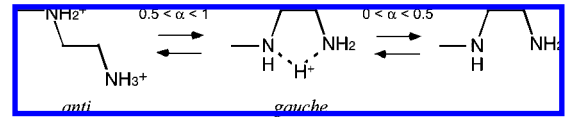

Preparation and Characterization of Polyplexes from PAsp(DET) and PAsp(DPT). The polyplex formation of PAsp(DET) and PAsp(DPT) was confirmed by agarose gel electrophoresis. The free pDNA band disappeared at N/P = 2 and 1.5 for PAsp(DET) and PAsp(DPT), respectively, indicating that all the pDNA molecules were associated with the polycations in the electrophoregram (Supporting Figure 2, Supporting Information). To quantitatively evaluate the relationship between N/P ratio and pDNA complexation with cationic PAsp(DET) and PAsp(DPT), an EtBr exclusion assay was completed. In this assay, pDNA complexation prevents EtBr molecules from intercalating into pDNA, resulting in the decrease in the EtBr fluorescence. Indeed, the EtBr fluorescence decreased with the increase in N/P ratios (Figure 2a), indicating the progressive complexation of pDNA with the polycations forming polyplexes. Also, Figure 2a exhibits that the inflection points of the fluorescence intensity are at N/P = 2 for PAsp(DET) and 1.4 for PAsp(DPT). These inflection points are in good agreement

(26) Corte, D. D.; Schelapfer, C.-W.; Daul, C. *Theor. Chem. Acc.* **2000**, *105*, 39–45.
(27) Bouchoux, G.; Choret, N.; Berruyer-Penaud, F. *J. Phys. Chem. A* **2001**, *105*, 3989–3994.

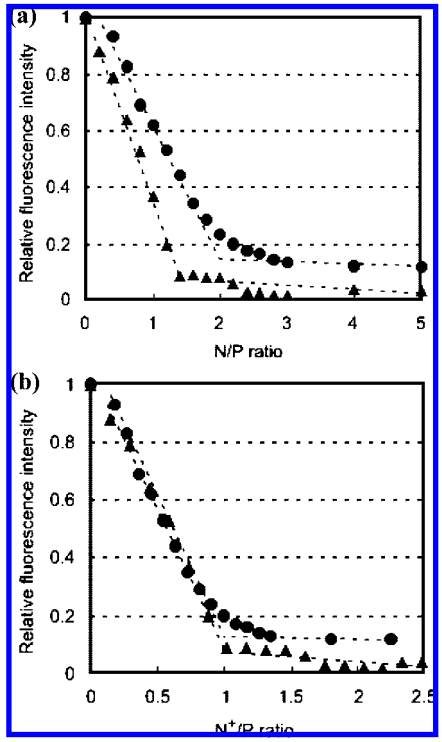

Figure 2. Ethidium bromide exclusion assay on PAsp(DET) and PAsp(DPT) polyplexes. (a) Relative fluorescence intensity vs N/P ratio. (b) Relative fluorescence intensity vs N^+/P ratio: (●) PAsp(DET) and (▲) PAsp(DPT).

with the N/P ratio where the free pDNA band disappeared from the electrophoregram (Supporting Figure 2, Supporting Information). These fluorescence data were replotted against N^+/P ratios, which were defined as the molar ratio of protonated amino groups at pH 7.4 in the polycations to phosphate groups in pDNA, as seen in Figure 2b. Note that the protonation degree of the amino groups of PAsp(DET) and PAsp(DPT) was determined to be 0.45 and 0.73 at pH 7.4, respectively, from the titration results without NaCl (data not shown). Obviously, both systems had the coincident inflection point of the fluorescence intensity at the N^+/P of unity, being consistent with the polyion-coupling between a phosphate group and an amino group in the protonated form expected from the α/pH curves. This result suggests that the pK_a value of PAsp(DET) shows minimal change with the polyplex formation, probably due to the thermodynamic penalty in diprotonated form of Asp(DET) units due to strong three-bond interaction (butane effect) caused by electrorepulsive interaction between two protonated amino groups.

The size and ζ-potential of polyplexes from PAsp(DET) and PAsp(DPT) in 10 mM Tris-HCl buffer (pH 7.4) were measured at 37 °C. As shown in Figure 3a, each polyplex had the critical range in N/P ratios, e.g., 2.5−3.5 and 1.4−1.5 for PAsp(DET) and PAsp(DPT), respectively, to reveal an appreciably large size of approximately 1000 nm. Considering that the ζ-potential of each polyplex was close to neutral in this critical range of N/P ratios, as seen in Figure 3b, these large-sized polyplexes may form through the secondary aggregation of the charge stoichiometric polyplexes showing minimal force of electrostatic repulsion. In the range over these critical N/P ratios, the size of both polyplexes were maintained <100 nm. The polyplexes in this range exhibited almost constant positive ζ-potential values (+30 mV) in both systems.

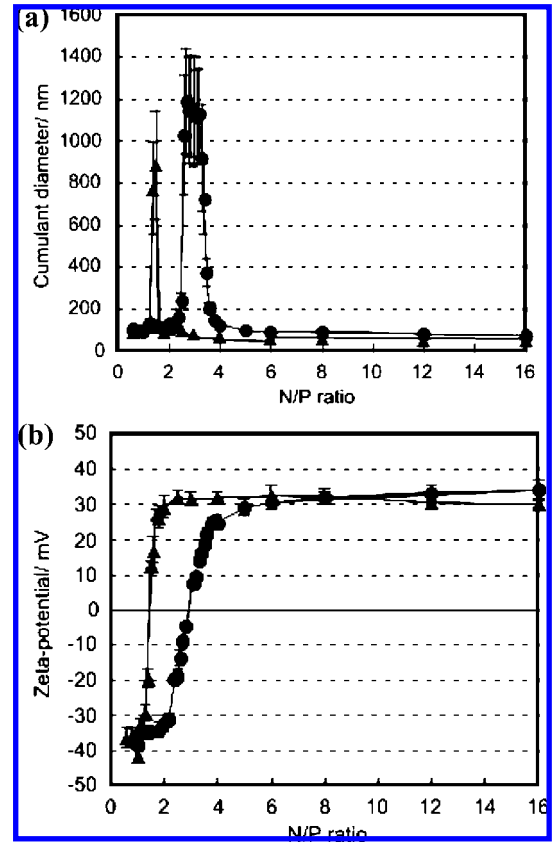

Figure 3. Change in the size and the ζ-potential of PAsp(DET) and PAsp(DPT) polyplexes with N/P ratio. (a) Cumulant diameter and (b) ζ-potential: (●) PAsp(DET), (▲) PAsp(DPT). All the samples were normalized to a concentration of 33 μg pDNA/mL at 37 °C. Results were expressed as mean ± SEM (n = 3).

Transfection Efficacy and Cytotoxicity of PAsp(DET) and PAsp(DPT) Polyplexes. The transfection efficacy of the luciferase gene against a human hepatocyte cell line (Huh-7) and a human umbilical vein endothelial cell (HUVEC) was compared between PAsp(DET) and PAsp(DPT) polyplexes. The polyplexes prepared at N/P ratios of 4, 8, and 16 were examined in this assay, having almost the same size and ζ-potential (Figure 3a,b). Polyplexes prepared from branched polyethylenimine (BPEI) (25 kDa) were used as a control. As seen in Figure 4a,b, the highest transfection efficacy in both cells was achieved by the PAsp(DET) polyplexes prepared at the N/P ratio of 16. This transfection efficacy of PAsp(DET) polyplexes was 1 order of magnitude higher than that of BPEI polyplexes against HUVEC. Obviously, the transfection efficacy of PAsp(DET) polyplexes was enhanced with the increase in N/P ratio against both cells. On the contrary, PAsp(DPT) exhibited the decrease in the transfection efficacy with the increase in N/P ratio. Considering that the large difference was not observed in the size and ζ-potential between PAsp(DET) and PAsp(DPT) polyplexes (Figure 3a,b), this opposite trend in transfection profiles of these two polyplexes against N/P ratio is likely to be due to the distinctive physicochemical properties directly related to the difference in the chemical structures, particularly the side chain structures. Interestingly, in the region of low N/P ratio, the PAsp(DPT) polyplexes revealed a comparable transfection efficacy to PAsp(DET) polyplexes, even though the former was expected to exert substantially weaker buffering capacity than the latter, as judged from the α/pH curve (Figure 1a).

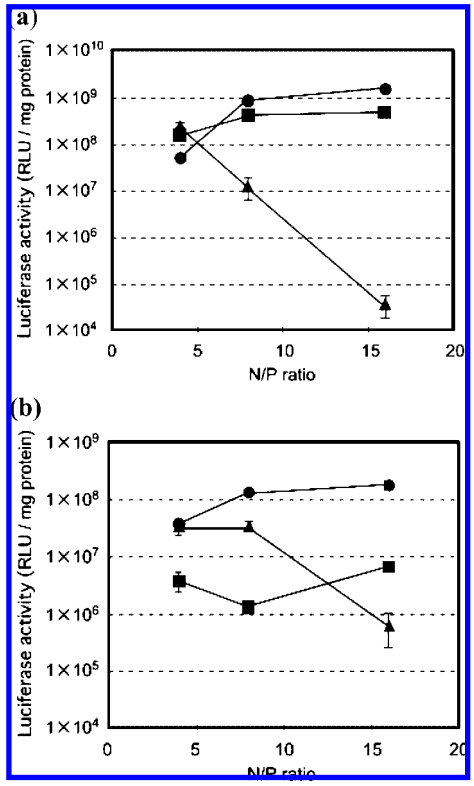

Figure 4. In vitro transfection of Huh-7 (a) and HUVEC (b) with PAsp(DET), PAsp(DPT), and BPEI polyplexes at varying N/P ratios evaluated by luciferase assays: (●) PAsp(DET), (▲) PAsp(DPT), and (■) BPEI. Results were expressed as mean ± SEM ($n = 4$).

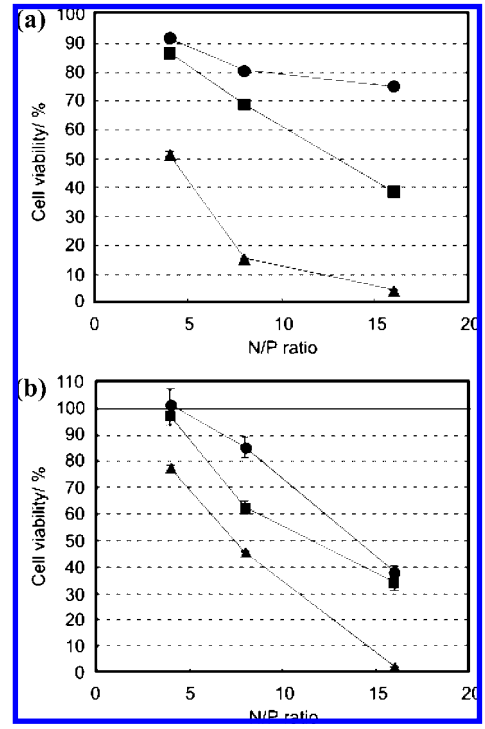

Figure 5. MTT cytotoxicity of Huh-7 (a) and HUVEC (b) with PAsp(DET), PAsp(DPT), and BPEI polyplexes evaluated under the same experimental conditions as in Figure 4 (luciferase assay): (●) PAsp(DET), (▲) PAsp(DPT), and (■) BPEI. Results were expressed as mean ± SEM ($n = 4$).

There are several key steps in the transfection process of an exogenous gene, such as cellular uptake, intracellular trafficking, release of the gene from the complexes, transcription, and translation. Furthermore, excess polycationic charge with polyplexes is an issue to induce impaired cellular homeostasis, resulting in the negative influences on whole transfection steps, especially transcription and translation. Indeed, our previous study revealed that the challenge of linear PEI polyplexes into Huh-7 cells stably expressing firefly luciferase highly impaired the transcription and translation processes to reduce the expression of firefly luciferase as well as a variety of house-keeping genes.[23] In this regard, a toxicological assay was completed to explore the different transfection profiles between PAsp(DET) and PAsp(DPT) polyplexes against N/P ratio. As shown in Figure 5a,b, the results of the MTT cell viability assay, the cytotoxicity of each polyplex under the same experimental condition as the luciferase assay increased with N/P ratio for both cells, Huh-7 and HUVEC. This result is in good agreement with the result from the MTT assay of each polymer without pDNA (Supporting Figure 3a,b and Supporting Table 1, Supporting Information). Obviously, the PAsp(DET) polyplex had much lower toxicity than the PAsp(DPT) polyplex. In detail, at a N/P ratio of 16 in Huh-7 cells, the viability of cells incubated with PAsp(DET) polyplexes was over 70% of that of control cells, whereas the viability was less than 10% in the case of PAsp(DPT) polyplexes (Figure 5a). Similarly, the cytotoxicity of PAsp(DPT) polyplexes was the highest against HUVEC, followed by BPEI and PAsp(DET) polyplexes (Figure 5b). From these results, it is worth noting that only one additional methylene group between two amino groups in the side chain crucially elevates the cytotoxicity of the cationic poly(aspartamides). This high cytotoxicity of PAsp(DPT) might contribute to the dramatically decreased transfection efficacy of PAsp(DPT) polyplexes at high N/P ratios. In contrast, cytotoxicity was substantially lowered in PAsp(DET) polyplexes, allowing high transfection efficacy with the increased N/P ratio.

To explore the endosomal escaping behavior of PAsp(DET) and PAsp(DPT) polyplexes, HUVEC trafficking studies were completed with a confocal laser scanning microscope (CLSM). In this experiment, pDNA was labeled by Cy5 (red), and nucleus and late-endosome/lysosome were stained by Hoechst 33342 (blue) and LysoTracker (green), respectively. Figure 6a,e shows the intracellular distribution of BPEI polyplexes 3 and 12 h after administration, respectively, as a positive control exerting an endosomal escaping function. Obviously, the red regions surrounding the yellow regions, where Cy5-labeled pDNA was localized in late-endosomes or lysosomes, were widely observed over time. It may be reasonable to judge that these spreading red regions represent the distribution of polyplexes exiting from the late endosomal or lysosomal stage into the cytoplasm. On the contrary, the negative control, PLys polyplexes, which lack significant buffering capacity, displayed much less red regions (Figure 6d,h), suggesting the segregation of Cy5-labeled pDNA in endo/lysosomal compartments without diffusing into cytoplasm. The confocal images of the cells transfected by PAsp(DET) polyplexes (Figure 6b,f) display spreading red regions into the cytoplasm, comparable to the previously described BPEI transfection. These data indicate facilitated transport of Cy5-labeled pDNA into the cytoplasm from the endo/lysosomal compartments. The CLSM images of PAsp(DET) polyplexes are consistent with the high buffering capacity of the native polymer. Interestingly, similar diffusing red regions were also observed for PAsp(DPT) polyplexes (Figure 6c,g), suggesting that PAsp(DPT) may facilitate endosomal escape of the polyplex, despite the previously determined poor pH-buffering capacity of PAsp(DPT). Indeed, PAsp(DPT) polyplexes showed

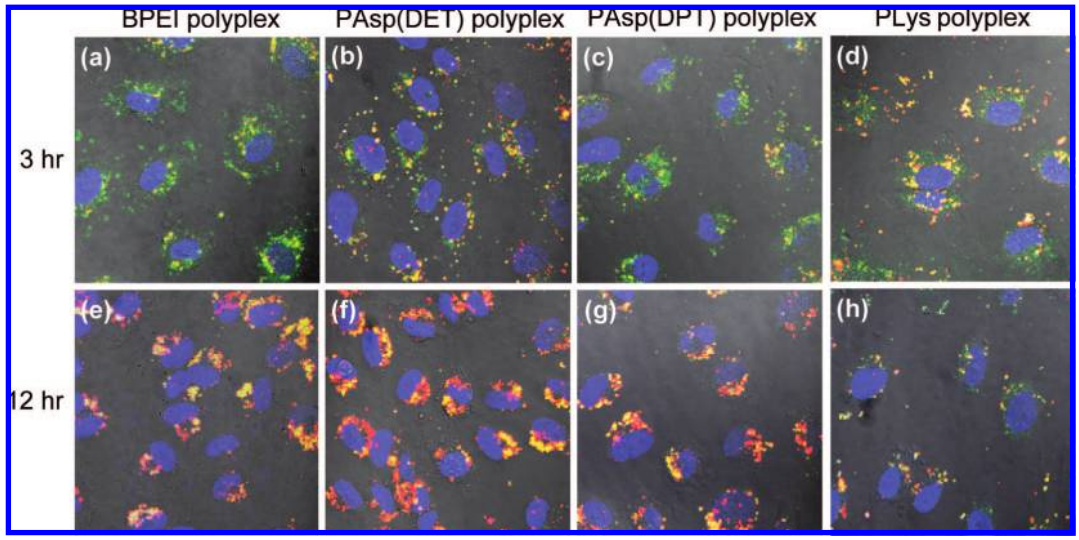

Figure 6. Intracellular distribution of Cy5-labeled pDNA complexed with a variety of polycations in HUVEC. Cy5-labeled pDNA and LysoTracker as a late-endosome and lysosome marker were observed in red and green, respectively. The cells were incubated at 37 °C for a definite time period, followed by washing with PBS, and subjected to CLSM imaging. Panels a−d and e−h are the images after 3 and 12 h incubation, respectively. (a and e) BPEI polyplexes (N/P = 8), (b and f) PAsp(DET) polyplexes (N/P = 8). (c and g) PAsp(DPT) polyplexes (N/P = 8). (d and h) PLys polyplexes (N/P = 2).

comparable transfection efficacy to BPEI and PAsp(DET) polyplexes at low N/P ratios (Figure 4a,b). These results strongly suggest the presence of another mechanism facilitating late endosomal or lysosomal escape beyond the putative proton sponge effect. Note that the medium change at 1 h after the polyplex administration significantly decreased the red regions (or dots) corresponding to endosomal escaping behavior in BPEI, PAsp(DET), and PAsp(DPT) (Supporting Figure 4, Supporting Information). This indicates that prolonged incubation of excess polyplexes with cells substantially facilitates the endosomal escape. Prolonged incubation should lead to the increased cellular uptake of polyplexes, presumably resulting in the polyplex accumulation with higher concentration in late-endosomal compartments to bring facilitated endosomal escape.

Membrane Destabilization by PAsp(DET) and PAsp(DPT). As described in the preceding section, the CLSM observation of Cy5-labeled pDNA in the intracellular compartment demonstrated that cytoplasmic transport efficiently occurred even for PAsp(DPT) polyplexes, known to possess the low buffering capacity. Of note, the previous studies addressed the destabilization of cellular membranes through the direct interaction with polycations,[5,6,28] possibly leading to the facilitated cytoplasmic transport of the polyplexes.[29−31] This destabilizing effect of polycations on the cellular membrane is considered to be dependent on the concentration (or N/P ratio), molecular weight, cationic charge density, and molecular structure of polycations.[5] Thus, the membrane destabilization induced by PAsp(DET) and PAsp(DPT) was estimated by the hemolysis assay, in which the amount of hemoglobin liberated from erythrocytes was determined from colorimetric analysis at 575 nm (Figure 7). Figure 7a clearly shows the significant difference in hemolytic activity between PAsp(DET) and PAsp(DPT) after an overnight incubation with murine erythrocytes at pH 7.4. The hemolytic activity of PAsp(DET) was negligible under the examined conditions, whereas PAsp(DPT) exhibited appreciable hemolytic activity in a concentration-dependent manner. Next, the hemolytic assays were repeated under acidic conditions indicative of the late endosomal or lysosomal state. Since overnight incubation of murine erythrocytes at pH 5.5 led to an appreciable decrease in the signal-to-noise ratio (Abs 575 nm), possibly due to instability of erythrocytes or conformational change of hemoglobins under the acidic condition, a shorter incubation time of 3 h was adopted. As clearly seen in Figure 7b, hemolytic activity levels were concentration-dependent for PAsp(DPT), regardless of the environmental pH. In direct contrast, however, the hemolytic activity of PAsp(DET) was critically enhanced by decreasing the environmental pH from 7.4 to 5.5 (Figure 7c), reaching the levels comparable to PAsp(DPT) (Figure 7b). The membrane destabilizing capacity of these polycations was further tested against HUVEC by a colorimetric LDH assay, in which the enzymatic activity of cytosolic LDH liberated from the cells was measured to estimate the membrane damages.[5,6] Figure 8a clearly shows that PAsp(DPT) induced LDH liberation in a concentration-dependent manner, both at acidic and physiological pH conditions. These data suggest a strong capacity of PAsp(DPT) to destabilize the endosomal membrane as well as the cytoplasmic membrane, regardless of the environmental pH. This is consistent with the results of the hemolysis assay shown in Figure 7b. Alternatively, the activity of LDH liberated from HUVEC incubated with PAsp(DET) was obviously low at pH 7.4, while the decrease in pH to acidic condition (pH ∼5) substantially enhanced its activity to the same level as that of PAsp(DPT) (Figure 8b), exhibiting the similar trend to the hemolytic activity (Figure 7c). Similar results of the membrane destabilization were obtained for Huh-7 cells (data not shown). Apparently, the concentration-dependent increase in the membrane destabilization capacity of PAsp(DET) under the acidic condition corresponds to the enhanced transfection efficacy with N/P ratios (Figure 4).

We next sought to find a correlation between the interaction of the polycations with the membrane and the destabilization effect. CLSM observations were further carried out for HUVEC

(28) Zhang, Z.-Y.; Smith, B. D. *Bioconjugate Chem.* **2000**, *11*, 805–814.
(29) Merdan, T.; Kunath, K.; Fischer, D.; Kopecek, J.; Kissel, T. *Pharm. Res.* **2002**, *19*, 140–146.
(30) Bieber, T.; Meissner, W.; Kostin, S.; Niemann, A.; Elsasser, H.-P. *J. Controlled Release* **2002**, *82*, 441–454.
(31) Walker, G. F.; Fella, C.; Pelisek, J.; Fahrmeir, J.; Boeckle, S.; Ogris, M.; Wagner, E. *Mol. Ther.* **2005**, *11*, 418–425.

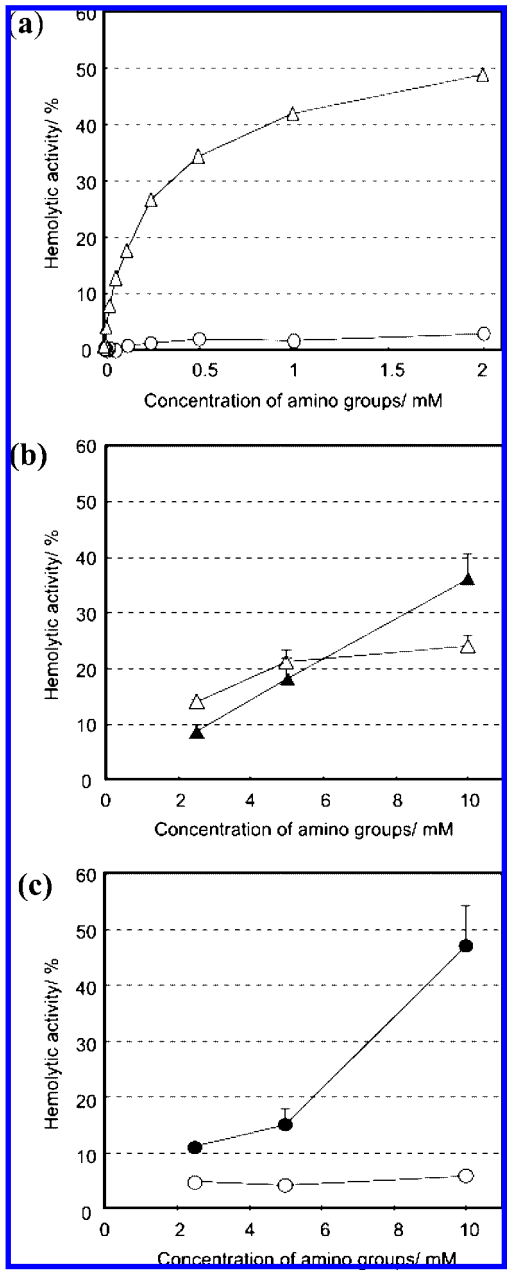

Figure 7. Hemolytic activity of PAsp(DET) and PAsp(DPT) against murine erythrocytes. (a) Hemolytic activity of PAsp(DET) (○) and PAsp(DPT) (△) after overnight erythrocyte incubation at pH 7.4 and 37 °C. (b) Hemolytic activity of PAsp(DPT) after 3 h incubation at pH 7.4 (△) and 5.5 (▲) (at 37 °C). (c) Hemolytic activity of PAsp(DET) after 3 h incubation at pH 7.4 (○) and 5.5 (●) (at 37 °C). Results were expressed as mean ± SEM ($n = 4$).

incubated with RhoB-labeled polycations. Fluorescence from PAsp(DET)−RhoB was not observed at pH 7.4 (Figure 9a) but upon acidic conditions (pH ∼5), the fluorescence intensity was significant, extending to the cell periphery (Figure 9b), thereby indicating the appreciable cellular association of PAsp(DET)−RhoB at the acidic pH. In addition, CLSM studies with PAsp(DPT)−RhoB clearly showed significant levels of fluorescence at both pH's (Figure 9c,d), indicating a strong associative behavior of PAsp(DPT)−RhoB to cellular membrane, regardless of the pH. These images are in good agreement with the membrane-destabilizing capacity of the polycations determined by the hemolysis and LDH assays (Figures 7 and 8). It is reasonable to conclude from these results that PAsp-

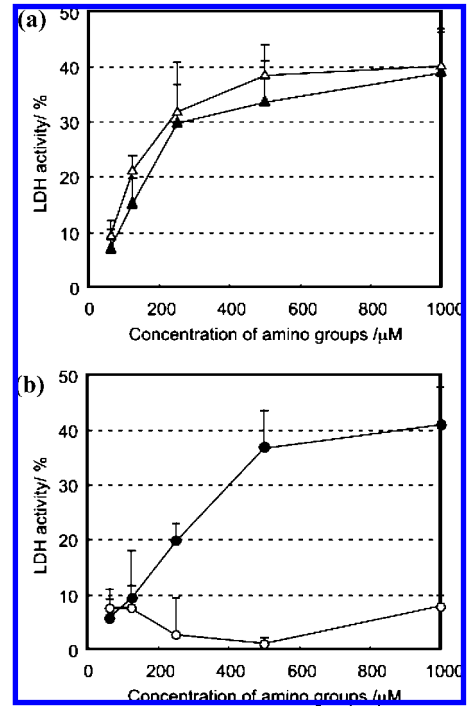

Figure 8. Enzymatic activity of LDH liberated from HUVEC upon interaction with the polycations at 37 °C for 1.5 h. (a) LDH activity for PAsp(DPT) system at pH 7.4 (△) and 5.5 (▲). (b) LDH activity for PAsp(DET) system at pH 7.4 (○) and 5.5 (●). Results were expressed as mean ± SEM ($n = 6$).

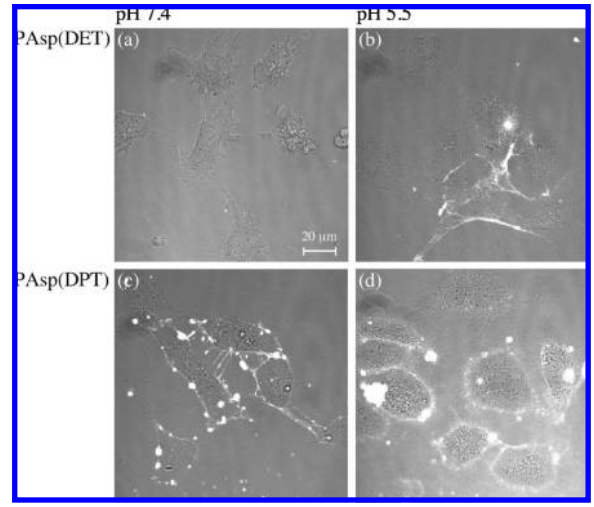

Figure 9. The adsorption of rhodamine B-labeled PAsp(DET) and PAsp(DPT) to HUVEC. The cells were incubated with the RhoB-labeled polycations (brightened as white) at the residual amino group concentration of 100 μM at 4 °C for 1 h, followed by washing with PBS, before CSLM imaging. (a) PAsp(DET) at pH 7.4, (b) PAsp(DET) at pH 5.5, (c) PAsp(DPT) at pH 7.4, (d) PAsp(DPT) at pH 5.5.

(DPT), without high buffering capacity (Figure 1), facilitates endosomal escape of its polyplexes into the cytoplasm through the direct perturbation of endosomal membrane. Nevertheless, the strong capacity of membrane destabilization, even at physiological pH, induces substantial damage to the cell membrane treated with PAsp(DPT) polyplexes as confirmed by the poor cell viability (Figure 5a,b). On the contrary, the weak interaction of PAsp(DET) with the plasma membrane at neutral pH is consistent with the lowered membrane-destabilizing capacity indicated from the results of hemolysis and LDH

assays. These data are supported by the high viability of the cells treated with PAsp(DET) polyplexes, as judged by MTT assay (Figures 5a,b). It should be further emphasized that the cellular association and the membrane-destabilizing capacity of PAsp(DET) were significantly enhanced by decreasing environmental pH to 5.5, becoming comparable to those of PAsp(DPT). This indicates that PAsp(DET) selectively destabilizes the membrane of the endosomal compartment with decreased pH to facilitate the endosomal escape of the polyplexes with minimal damage to the plasma membrane facing an extracellular pH of 7.4. Furthermore, it is reasonable to assume that cytoplasmic PAsp(DET) polyplexes may show minimal interaction with the membranes of organelles because of the pH recovery from acidic to neutral accompanied by the migration from the endosome to cytoplasm. Eventually, PAsp(DET) polyplexes successfully achieved the high transfection efficacy without impairing the cellular viability, as seen in Figure 4.

The unique pH dependency of the affinity of PAsp(DET) to cellular membrane is apparently correlated with the two-step protonation behavior of the flanking 1,2-diaminoethane unit in PAsp(DET). As described in the former section, the 1,2-diaminoethane unit assumes a monoprotonated gauche form at neutral pH, while additional protonation at an acidic pH induces a conformational transition to a diprotonated anti form (Scheme 1). This protonation change accompanying the conformational transition is likely related with the pH-modulated interaction of PAsp(DET) with the cellular membrane. Apparently, PAsp(DET) with the diamine unit in the monoprotonated gauche state exhibited a weak affinity for the cellular membrane but the diprotonated anti state revealed an increased affinity to perturb the membrane integrity. In contrast, the 1,3-diaminopropane unit in PAsp(DPT) assumes a diprotonated form at physiological, late endosomal, and lysosomal pH conditions; moreover, PAsp(DPT) shows a strong interaction with the cellular membrane, even at neutral pH conditions.

Conclusion

The present study was devoted to clarify key chemical parameters for the next generation of polycation/polyplexes exhibiting augmented levels of transfection efficacy and negligible cytotoxicity both in vitro and in vivo. This work primarily focused on N-substituted cationic poly(aspartamide) derivatives, PAsp(DET), possessing flanking 1,2-diaminoethane side chain, previously identified for effective in vivo transfection.[15,16] Comparative analysis between PAsp(DET) and PAsp(DPT) revealed that a single methylene unit difference in the diamine side chains had a crucial effect on the multiple cationic charge states. This seemingly minimal chemical change produced a striking contrast in their polyplex transfection behaviors, presumably due to the increased cytotoxicity. The high cytotoxicity of PAsp(DPT) was closely correlated to the degree of membrane destabilization, which was consistent with the strong interaction of PAsp(DPT) with the cellular membrane, even at physiological pH. The results of CLSM, hemolysis, and LDH analysis indicate that the membrane-destabilizing capacity of PAsp(DPT) contributes to the intracellular transport of PAsp(DPT) polyplexes, despite its weak buffering capacity. In contrast, the membrane destabilizing capacity of PAsp(DET) was highly altered, depending on the environmental pH. Two cationic charge states emerged with a monoprotonation at neutral pH and a diprotonated state at acidic conditions. We conclude that PAsp(DET) exhibits pH-selective membrane destabilization for late endosomal or lysosomal escape without compromising the membrane integrity of cytoplasmic vesicles and/or organelles. This unique approach provides the impetus for future nonviral gene vector development from synthetic poly(amino acids) with facile insertion of pH-selective membrane destabilizing structures to augment transfection efficacy and limit cytotoxicity. Thus, we show a novel and effective method to construct smart carrier systems useful for intracellular delivery of versatile bioactive components with inherently poor permeability to cellular membranes.

Acknowledgment. This work was financially supported by the Core Research Program for Evolutional Science and Technology (CREST) from the Japan Science and Technology Corp. (JST) as well as by Special Coordination Funds for Promoting Science and Technology from the Ministry of Education, Culture, Sports, Science and Technology of Japan (MEXT). The authors express their appreciation to Dr. H. Hamada (RIKEN, Japan) for providing the plasmid DNA and Dr. Darin Y Furgeson (University of Wisconsin—Madison) for proofreading of the manuscript. K. Miyata thanks the Research Fellowships of the Japan Society for the Promotion of Science for Young Scientists (JSPS) and the Mitsubishi Chemical Corp. Fund for their financial support.

Supporting Information Available: Experimental Section, Supporting Scheme 1, Supporting Figures 1−4, and Supporting Table 1. This material is available free of charge via the Internet at http://pubs.acs.org.

JA804561G